

Miniaturized Implantable Loop Antenna for Biomedical Applications

Dr. S. Suganthi, M. Noorjahan

Dept. of ECE, K.Ramakrishnan College of Technology, Trichy, TamilNadu, India

Dr. P. Thiruvalar Selvan

Dept. of ECE, TRP Engineering College, Trichy, TamilNadu, India

Abstract— An implantable loop antenna is proposed for biomedical applications. The size of the proposed antenna is $13 \times 13 \times 1.27 \text{ mm}^3$ is obtained. The proper feed and short pins for obtaining either RHCP or LHCP property can be realized. The proposed antenna is designed for Industrial, Scientific and Medical (ISM) (2-2.48 GHz) biomedical applications. The return loss of the loop antenna can be realized with S_{11} less than -10 dB and axial ratio below 3 dB.

Keywords— Miniature antenna, Industrial, Scientific and Medical (ISM) band, RHCP, LHCP, implantable antenna.

I. INTRODUCTION

Because of the rapid development of ultra wide band communication systems in recent years, much research has been conducted on UWB antennas, among which printed wide aperture antennas have been regarded as popular candidates. The frequency range for UWB systems between 3.1–10.6 GHz will cause interference to the existing wireless communication systems, such as the wireless local area network (WLAN) for IEEE 802.11a operating in 5.15–5.35 and 5.725–5.825 GHz bands, WiMAX (3.3–3.6 GHz), and C-band (3.7–4.2 GHz), so the UWB antenna with single and dual band-stop performances is required.

In order to satisfy IEEE 802.11 a standard, the proposed antenna should operate at 2.45 GHz. [1]. Therefore, slotted antennas for WLAN applications become a research point [2] in the past decades and many different technologies for miniaturized antenna have been proposed. The 915MHz ISM band (902MHz ~ 928MHz) is a commonly used unlicensed band in the United States of America and 2.4GHz ISM band [3] (2.402GHz ~ 2.484GHz) is the most commonly used unlicensed band [4] worldwide for industrial, scientific, and medical applications. Demand for compact antennas operating in ISM bands is increasing day by day.

Some designs with dual band-notched property are achieved by utilizing a couple of half-wavelength parasitic elements [5] in an open rectangular slot, embedding dual C-shaped slots on the radiator or inserting dual quarter-wavelength stubs[6]. However, the above designs have limited band-notched performance ($VSWR < 10$) [7] at each notched frequency or limited gain suppression ($< 10 \text{ dB}$) in the notched band. However, it had limited band [8] performance due to the dielectric loss of the substrate. Another method was suggested in which had introduced a substrate integrated waveguide [9] (SIW) cavity within the feed line of a monopole antenna [10] to obtain multiple band-notched functions. In constructing an implantable antenna, it

is critical to place the implant in the medium in which it operates. In this paper, an implantable antenna is proposed for industrial, scientific, and medical (ISM) applications. The proposed antenna is found to be compact in size and has a reasonable return loss of -10 dB to cover the ISM band, which is insensitive to the variation of the electrical properties of the human body.

Only a few implantable antennas have been evaluated under the ISM band and the proposed system is mainly tested for ISM band applications. Since large implants are used to reduce the transmission range, we are forced to construct compact antennas for adequate use in the ISM band since human skin and body fluids are strong attenuators of signals.

A coplanar waveguide (CPW) fabricated on a dielectric substrate was first demonstrated by C. P. Wen [2] [3] [4] [11]. Since that time, tremendous progress has been made in CPW based microwave integrated circuits (MICs) as well as monolithic microwave integrated circuits (MMICs) [12] - [13]. The advantages of a coplanar waveguide structures over the conventional microstrip lines [14] are: Firstly fabrication process is simplified in CPW-fed structures. Secondly, it facilitates easy shunt as well as series surface mounting of active devices. Third, it eliminates the need for wrap around and via holes, and fourth, it reduces radiation loss.

Furthermore the characteristic impedance is determined by the ratio of the dimensions, so size reduction is possible without limit, at the cost of higher losses. Also, there exists a ground plane between any two adjacent lines; hence cross talk effects between adjacent lines are very weak.

Major advantages gained in manufacturing are, first, CPW lends itself to the use of automatic pick-and-place and bond assembly equipments for surface mount component placement and interconnection of components, respectively [15]. Second, CPW allows the use of computer controlled on wafer measurement techniques for device and circuit characterization up to several tens of GHz [16], [17].

These advantages make CPW [18, 19] based MICs and MMICs cost effective in large volume. As a result, CPW circuits can be made denser than conventional microstrip circuits. These features make CPW ideally suited for Microwave integrated circuits as well as Monolithic microwave integrated circuits applications. The quasi-TEM mode of propagation [20, 21] on a CPW has low dispersion and hence offers the potential to construct wide band circuits and components.

II. ANTENNA DESIGN

The main dimensions of antenna are listed in Table I.

1. Width of the patch

$$\frac{C}{2f_0} \sqrt{\frac{2}{\epsilon_r + 1}} \tag{1}$$

λ is wavelength

C is Velocity of light ($3 * 10^8$ m/s)

f_0 is Operating/ Resonant frequency (in GHz)

2. Length of the patch

$$\epsilon_{r_{eff}} = \frac{\epsilon_r + 1}{2} + \frac{\epsilon_r - 1}{2} \left[1 + 12 \frac{h}{W} \right]^{-1/2} \tag{2}$$

Where, ϵ_r is the relative permittivity of the substrate

h is the thickness of the substrate and is given by

$$h = \frac{0.0606\lambda}{\sqrt{\epsilon_r}} \tag{3}$$

The incremental length of the patch [22,23] along its length has now been extended on each end by a distance ΔL and is given by empirical formula (Ramesh et al, 2001)

$$\Delta L = 0.412h * \frac{(\epsilon_{eff} + 0.3) * \left(\frac{W}{h} + 0.264\right)}{(\epsilon_{eff} - 0.258) * \left(\frac{W}{h} + 0.8\right)} \tag{4}$$

The effective length is

$$L_{eff} = \frac{C}{2f_0 \sqrt{\epsilon_{eff}}} \tag{5}$$

The length of the patch is finally given as

$$L = L_{eff} - 2\Delta L \tag{6}$$

3. The fed location design

The position of the fed can be obtained by using (Dr.Max Ammann)

$$X_f = \frac{L}{\sqrt{\epsilon_{r_{eff}}}} \tag{7}$$

Where X_f is the desire input impedance to match the fed and $\epsilon_{r_{eff}}$ is the effective dielectric constant.

$$Y_f = \frac{W}{2} \tag{8}$$

4. Ground dimension

For practical consideration, it is essential to have a finite ground plane if the size of the ground plane is greater than the patch dimensions by approximately six times the substrate thickness all around the periphery. Hence, the ground plane dimensions would be given as (Huang, 1983) (Thomas, 2005)

$$L_g = 6h + L; W_g = 6h + L; \tag{9}$$

The geometry of the antennas in this section was decided by the parametric study of each element in the software. The proposed implantable antenna consist of substrate, superstrate has the thickness of 1.27 mm and each having the thickness of 0.635 mm. The basic antenna structure consists of a square radiating patch, a feed line, and a ground plane. The patch is connected to a feed line. On the other side of the substrate, a conducting ground plane is placed.

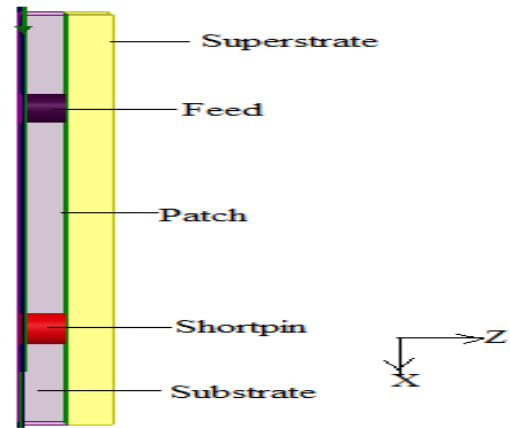


Fig.1: Side view of the antenna

In Fig 2 the antenna is intended to be implanted into a skin environment. Because the skin have a large dielectric constant than fat, they contribute more in reducing the size of the implant antenna. When comparing skin with muscle, it is quite obvious that an implantable antenna placed in the skin, minimizing the power loss caused by the tissue. The antenna is placed inside the skin environment in the depth of $h=3$ mm. The antenna is designed on Rogers 3010 substrate with dielectric constant 10.2 and loss tangent $\tan \delta = 0.0035$ and height $h= 0.635$.

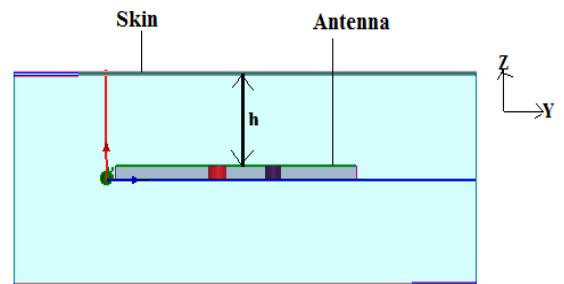


Fig.2: Antenna inside the skin environment

Fig. 3 shows the the implantable loop antenna structure. The proposed loop antenna consist of four small patches are connected to the loop with four high impedance lines separately at different quadrants. Two shorting pins with diameter of 0.9 mm are located at quadrant I and III, separately. The proposed antenna is fed at quadrant IV. A short pin is also used to assist in antenna miniaturization. The pin behaves like a ground plane increases the electrical length of the antenna.

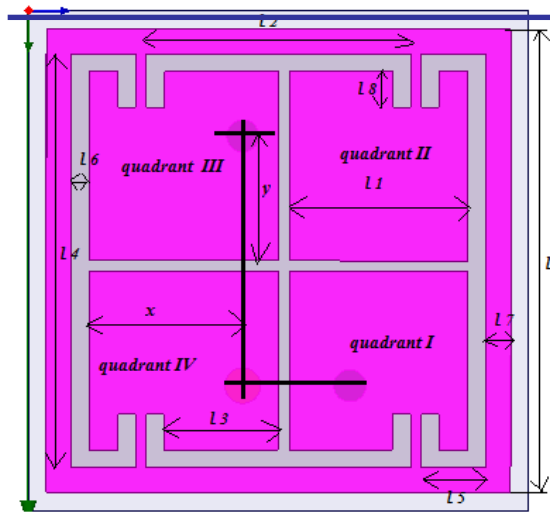


Fig.3: Geometry of the antenna

TABLE I DIMENSIONS OF THE PROPOSED ANTENNA (mm)

Parameters	Dimensions(mm)
L	13
l_1	5.15
l_2	7.4
l_3	3.05
l_4	11.6
l_5	1.8
l_6	0.5
l_7	0.7
l_8	1.5
X	5
Y	3.35

The proposed antenna is designed using the EM simulator HFSS. In order to calculate the full three-dimensional electromagnetic field inside a structure and the corresponding S-parameters, HFSS employs the finite element method (FEM). FEM is a very powerful tool for solving complex engineering problems, the mathematical formulation of which is not only challenging but also tedious. The basic approach of this method is to divide a complex structure into smaller sections of finite dimensions known as elements. These elements are connected to each other via joints called nodes. Each unique element is then solved independently of the others thereby drastically reducing the solution complexity. The final solution is then computed by reconnecting all the elements and combining their solutions. These processes are named assembly and solution respectively in the FEM.

III. RESULTS AND DISCUSSION

The simulated return loss graph is shown in figure. 4. It is therefore important to refine at a frequency for which the return loss is high and hence the mesh refinement can produce

accurate results. Various cases were simulated in order to investigate how this parameter affects the results in HFSS. The value of delta S, which was common to all of them, was specified as 0.02. Return is the loss of signal power resulting from the reflection caused at a discontinuity in a transmission line. The simulated return loss graph covers the ISM band range

Return loss= $-20 \log |S_{11}|$ dB

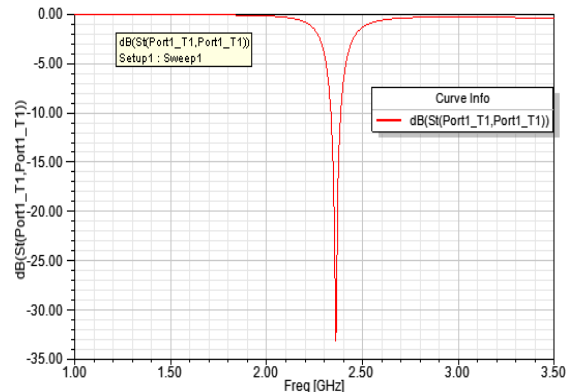


Fig.4: Simulated return loss S_{11}

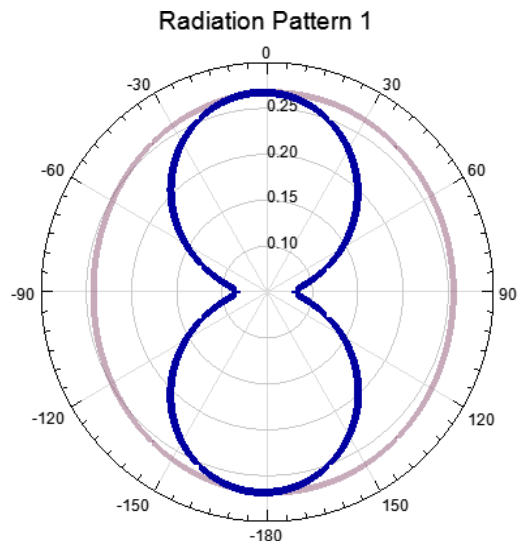


Fig 5: Simulated radiation patterns of Antenna at 2.4GHz

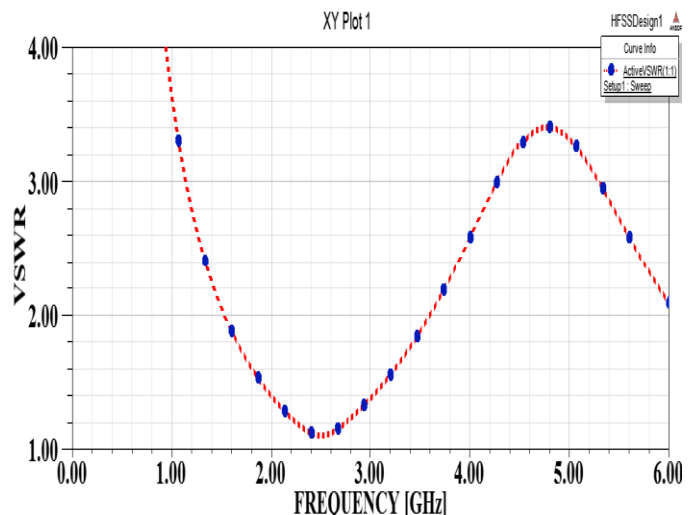


Fig .6. VSWR of the proposed antenna

Fig. 5 A relatively good radiation efficiency (radiated to net input power ratio) is obtained for the antenna in this simulation setup. Figure 5 presents the simulated radiation efficiency of the antenna. The radiation efficiency of the antenna is about 50% to 60%. It can be seen that although the efficiency shows some level of decrease with the improvement of impedance bandwidth, it is acceptable for the circularly polarized antenna. Radiation pattern shown in below figures presents the graphical representation of radiation properties of antenna as a function of space co-ordinates taken in xy plane. The proposed antenna has bi-directional radiation patterns in E-plane at 2.4 GHz resonant frequency. In H-plane, the antenna has Omni-directional radiation patterns, which indicates that it can receive the signals in all directions.

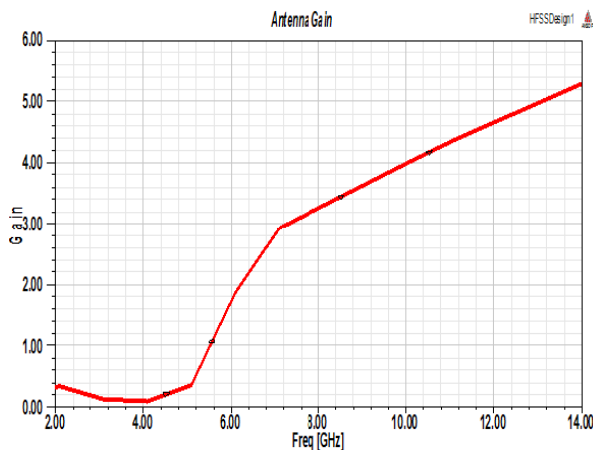


Fig 7. Gain of the proposed antenna

III CONCLUSION

In this paper Circular polarized implantable antenna. The design was performed while the antenna was placed in the skin environment. Furthermore, the same size of proposed antenna is suitable for implanting into muscle, heart or eye tissue and it satisfies the return loss of -10 db in the ISM band. The design antenna exhibits a good impedance matching of approximately 50 Ω . This antenna can be easily fabricated on substrate material due to its small size and thickness. The simple feeding technique used for the design of this antenna makes this antenna a good choice in many communications.

REFERENCES

- [1]. C. A. Balanis, *Antenna Theory: Analysis and Design*, 2nd Ed. Wiley India Pvt. Limited, 2007.
- [2]. Kang Ding, Yong-Xin Guo, *Senior Member, IEEE*, and Cheng Gao, *Member, IEEE* CPW-Fed Wideband Circularly Polarized Printed Monopole Antenna with Open Loop and Asymmetric Ground Plane. 2016.
- [3]. You-Jhu Chen, Te-Wei Liu, and Wen-Hua Tu, *Senior Member, IEEE* CPW-Fed Penta-Band Slot Dipole Antenna Based on Comb-Like Metal Sheets. 2016.
- [4]. Slawomir Koziel, *Senior Member, IEEE*, and Adrian Bekasiewicz A Structure and Simulation-Driven Design of Compact CPW-Fed UWB Antenna. 2016.
- [5]. J. Y. Sze, and J. Y. Shiu, "Design of band notched ultrawideband square aperture antenna with a hat-shaped back-patch," *IEEE Trans. Antennas Propag.*, vol. 56, no. 10, 2008, pp. 3311-314.
- [6]. Y. C. Lin, and K. J. Hung, "Compact ultra-wideband rectangular aperture antenna and band-notched designs," *IEEE Trans. Antennas Propag.*, vol. 54, no. 11, 2006, pp. 3075-3081.
- [7]. C. Y. Huang, W. C. Hsia, and J. S. Kuo, "Planar ultra-wideband antenna with a band-notched characteristic," *Microwave Opt. Technol. Lett.*, vol. 48, no. 1, 2005, pp. 99-101.
- [8]. A. M. Abbosh, M. E. Bialkowski, J. Mazierska, and M. V. Jacob, "A planar UWB antenna with signal rejection capability in the 4-6 GHz band," *IEEE Microw. Wireless Compon. Lett.*, vol. 16, no. 5, 2006.
- [9]. Z. A. Zheng, Q. X. Chu, and Z. H. Tu, "Compact band-rejected ultrawideband slot antennas inserting with $\lambda/2$ and $\lambda/4$ resonators," *IEEE Trans. Antennas Propag.*, vol. 59, no. 2, 2011, pp. 90-97.
- [10]. I. J. Yoon, H. Kim, H. K. Yoon, Y. J. Yoon, and Y. H. Kim, "Ultra-wideband tapered slot antenna with band cutoff characteristic," *Electron. Lett.*, vol. 41, no. 11, 2005, pp. 629-630.
- [11]. K. H. Kim, Y. J. Cho, S. H. Hwang, and S. O. Park, "Band-notched UWB planar monopole antenna with two parasitic patches," *Electron. Lett.*, vol. 41, no. 14, 2005, pp. 783-784.
- [12]. K. H. Kim, and S. O. Park, "Analysis of the small band-rejected antenna with the parasitic strip for UWB," *IEEE Trans. Antennas Propag.*, vol. 54, no. 6, 2006, pp. 1688-1692.
- [13]. P. Li, J. Liang, and X. D. Chen, "Study of printed elliptical/circular slot antennas for ultrawideband applications," *IEEE Trans. Antennas Propag.*, vol. 54, no. 6, 2006, pp. 1670-1675.
- [14]. C. P. Wen, "Coplanar Waveguide: A Surface Strip Transmission Line Suitable for Nonreciprocal Gyromagnetic Device Applications," *IEEE Trans. Microwave Theory Tech.*, Vol. 17, No. 12, pp. 1087-1090, Dec. 1969.
- [15]. J. L. B. Walker, "A Survey of European Activity on Coplanar Waveguide," 1993 IEEE MTT-S Int. Microwave Symp. Dig., Vol. 2, pp. 693 - 696, Atlanta, Georgia, June 14 -18, 1993.
- [16]. T. Sporkmann, "the Current State of the Art in Coplanar MMICs," *Microwave J.*, Vol. 41, No. 8, pp. 60 - 74, Aug. 1998.
- [17]. R. N. Simons, "Coplanar Waveguide Circuits. Components and Systems," New York: John Wiley and Sons, pp. 351-360, 2001.
- [18]. J. Browne, "Broadband Amps Sport Coplanar Waveguide," *Microwaves RF*, Vol. 26, No. 2, pp. 131 — 134, Feb. 1987.
- [19]. S. Suganthi, "Double folded multiband slot antenna with dual E shaped stub", Proc. ICEET'16, Indira Ganesan College of Engineering, 19th March, 2016
- [20]. S. Suganthi, "Multiband planar MIMO antenna for GSM1800/LTE2300/WIMAX/WLAN applications" Fourth National Conference on Innovation in Computing and Communication Technology" in Kongunadu College of Engineering and Technology, March 25, 2016.
- [21]. E.M. Godshalk and J. Pence, "Low-Cost Wafer Probe Scales 110-GHz Summit," *Microwaves RF*, Vol. 32, No. 3, pp. 162- 167, March 1993.
- [22]. S. M. J. Liu and G. G. Boll, "A New Probe for W-band On-wafer Measurements," 1993 IEEE MTT-S Int. Microwave Symp., Dig., Vol. 3, pp. 1335—1338, Atlanta, Georgia, June 14-18, 1993.
- [23]. S. Suganthi, "Compact MIMO antenna for portable devices in UWB applications" Proc. Indian Antenna Week 2016, Thiagarajar College of Engineering, Madurai, 6th June, 2016.